


Hidden antiferromagnetic order in Fe-based superconductor BaFe<sub>2</sub>As<sub>2</sub> and NaFeAs above T<sub>S</sub>Seiichiro Onari  and Hiroshi Kontani

Department of Physics, Nagoya University, Furo-cho, Nagoya 464-8602, Japan

 (Received 25 November 2019; revised 8 April 2020; accepted 21 September 2020; published 12 October 2020)

In several Fe-based superconductors, slight C<sub>4</sub> symmetry breaking occurs at T\*, which is tens of degrees Kelvin higher than the structural transition temperature T<sub>S</sub>. In this “hidden” nematic state at T<sub>S</sub> < T < T\*, the orthorhombicity is tiny [ $\phi = (a - b)/(a + b) \ll 0.1\%$ ], but clear evidence of a bulk phase transition has been accumulated. To explain this long-standing mystery, we propose the emergence of antiferro-bond (AFB) order with the AF wave vector  $\mathbf{q} = (0, \pi)$  at T = T\*, by which the characteristic phenomena below T\* are satisfactorily explained. This AFB order originates from the interorbital nesting between the d<sub>xy</sub>-orbital hole pocket and the electron pocket, and this interorbital bond order naturally explains the pseudogap, band folding, and tiny nematicity that is linear in T\* - T. The hidden AFB order explains key experiments in both BaFe<sub>2</sub>As<sub>2</sub> and NaFeAs, but it is not expected to occur in FeSe because of the absence of the d<sub>xy</sub>-orbital hole pocket.

DOI: [10.1103/PhysRevResearch.2.042005](https://doi.org/10.1103/PhysRevResearch.2.042005)

The emergence of rich nematic phase transitions is a central unsolved issue in Fe-based superconductors. At the structural transition temperature T<sub>S</sub>, ferro-orbital (FO) order with  $\psi \equiv (n_{xz} - n_{yz})/(n_{xz} + n_{yz}) \neq 0$  is driven by electron correlation [1], by which the orthorhombicity  $\phi = (a - b)/(a + b)$  occurs in proportion to  $\psi$ . Above T<sub>S</sub>, the electronic nematic susceptibility develops divergently [2–5]. As possible mechanisms of nematicity, both spin-nematic scenarios [6–12] and the orbital/charge-order scenarios [13–24] have been proposed. Both scenarios were successfully applied to the nematicity in BaTi<sub>2</sub>Sb<sub>2</sub>O [25–27] and cuprate superconductors [28].

However, the nematicity in Fe-based superconductors recently exhibited a very rich variety beyond the original expectation. Well-known discoveries are nematicity without magnetization in FeSe and nematicity with B<sub>2g</sub> symmetry in the heavily hole-doped compound AFe<sub>2</sub>As<sub>2</sub> (A = Cs, Rb) [29–33], which is rotated by 45° with respect to the nematicity in FeSe. These nematic orders are naturally understood as the ferro-orbital and/or bond orders driven by the interference between spin fluctuations described in Fig. 1(a) [17], where C<sub>Q<sub>s</sub></sub>, Q<sub>s</sub> gives the three-boson coupling.

The most significant open issue in the nematicity is the emergence of another type of nematicity in various Ba122 compounds below T = T\*, which is higher than T<sub>S</sub> by tens of degrees Kelvin. A true second-order bulk nematic transition at T\* has been reported in many experimental studies, such as a magnetic torque study [34], an x-ray study [35], an optical measurement study [36], and a laser photoemission electron microscope study [37].

Below T\*, the orthorhombicity  $\phi$  is finite but very small ( $\ll 0.1\%$ ), but a sizable pseudogap and shadow band exist [38,39]. The exponent of the nematicity  $\psi \propto \phi \propto (T^* - T)^\alpha$  is  $\alpha \sim 1$ , which is much larger than the mean-field exponent (1/2). The relation  $\phi \propto (T^* - T)$  is also observed in NaFeAs [40]. One may consider that the nematicity at T\* is not a true phase transition but that it reflects the inhomogeneity of the FO-order transition temperature T<sub>S</sub> due to local uniaxial pressure and randomness [7,41,42]. On the other hand, T\* seems not to be sensitive to the sample quality, and the domain structure of nematicity observed in the C<sub>4</sub> phase above T<sub>S</sub> [36,37] is homogeneous. The aim of this study is to reveal the origin of this mysterious hidden nematic state below T = T\* and to explain why multistage-nematic transitions (at T = T\* and T<sub>S</sub>) emerge in Ba122 and NaFeAs families.

In this Rapid Communication, we predict the emergence of antiferro-bond (AFB) order with the AF wave vector  $\mathbf{q} = (0, \pi)$  at T = T\* above the FO-order transition temperature T<sub>S</sub>. Below T\*, the AFB order causes a pseudogap in the density of states and a small T-linear nematicity  $\psi \propto T^* - T$ . The AFB order does not interrupt the ferro-orbital order at T<sub>S</sub>, because these order parameters have different orbital components. Thus, both the spin and nematic susceptibilities,  $\chi^s(\mathbf{Q})$  and  $\chi_{\text{nem}}(\mathbf{0})$ , respectively, show only a small anomaly at T = T\*. The obtained interorbital AFB order is driven by the interference between antiferro- and ferro-spin fluctuations, which are caused by the interorbital nesting between the d<sub>xy</sub>-orbital hole pocket and electron pockets. The present theory naturally explains the long-standing mystery of the hidden nematic state below T\* in Ba122 and NaFeAs families, in both of which T-linear nematicity has been reported [34,40].

In contrast, the AFB order does not occur in the FeSe model that has no d<sub>xy</sub>-orbital hole pocket, since the interorbital nesting is essential to realize the AFB order. This result is consistent with the absence of T\* in FeSe [43].

Below, we denote the five d orbitals d<sub>3z<sup>2</sup>-r<sup>2</sup></sub>, d<sub>xz</sub>, d<sub>yz</sub>, d<sub>xy</sub>, and d<sub>x<sup>2</sup>-y<sup>2</sup></sub> as l = 1, 2, 3, 4, and 5, respectively. We analyze the

Published by the American Physical Society under the terms of the [Creative Commons Attribution 4.0 International license](https://creativecommons.org/licenses/by/4.0/). Further distribution of this work must maintain attribution to the author(s) and the published article's title, journal citation, and DOI.

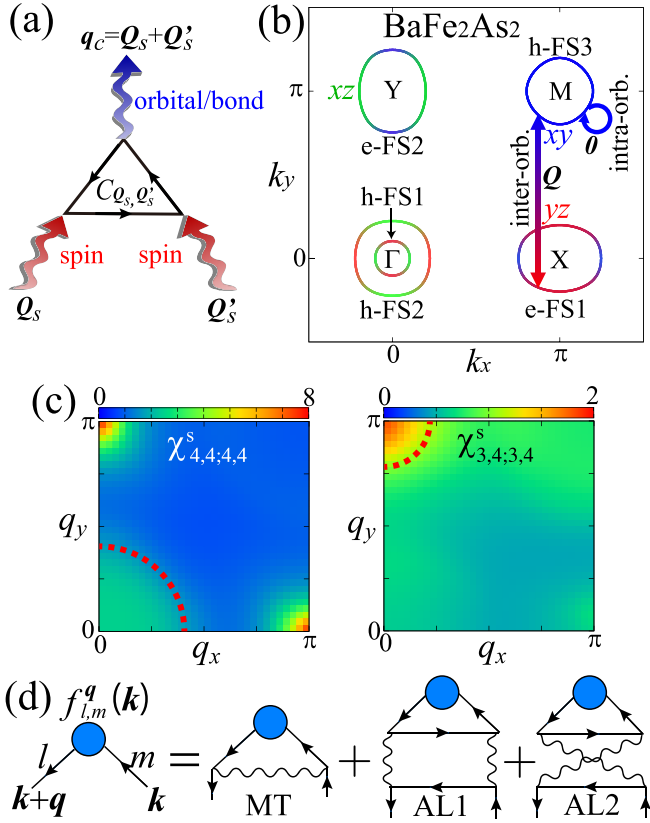


FIG. 1. (a) Quantum process of the spin-fluctuation-driven orbital fluctuations with  $q_c = Q_s + Q'_s$ . (b) FSs of the BaFe<sub>2</sub>As<sub>2</sub> model in the unfolded zone. The colors green, red, and blue correspond to orbitals 2, 3, and 4, respectively. (c)  $q$  dependences of  $\chi^s_{4,4;4,4}(q, 0)$  and  $\chi^s_{3,4;3,4}(q, 0)$  given by the RPA. The large antiferro- and ferro-fluctuations shown by dotted circles are significant for the AFB order formation. (d) Feynman diagrams of the DW equation. Each wavy line represents a fluctuation-mediated interaction.

following two-dimensional eight-orbital  $d$ - $p$  Hubbard model with parameter  $r$  [19],

$$H_M(r) = H^0 + rH^U, \quad (1)$$

where  $H^0$  is the unfolded tight-binding model for BaFe<sub>2</sub>As<sub>2</sub> [44], FeSe [19], and NaFeAs; more details are presented in Supplemental Material (SM) A [45].  $H^U$  is the first-principles screened  $d$ -electron Coulomb potential in each compound [46], and  $r$  is the reduction parameter, which is approximately proportional to the renormalization factor  $z$  in the coherence part of the Green's function [20]. We note that  $r$  is the unique free parameter in the present theory. We set  $r$  to reproduce experimental weak (FeSe) or moderate (NaFeAs, BaFe<sub>2</sub>As<sub>2</sub>) spin fluctuation strengths in the random phase approximation (RPA).

First, we focus on the unfolded BaFe<sub>2</sub>As<sub>2</sub> model directly given by the first-principles calculation using WIEN2K. Figure 1(b) shows the unfolded Fermi surfaces (FSs). The size of h-FS3 around the  $M$  point composed of orbital 4 is similar to that of e-FS1(2) around the  $X$ ( $Y$ ) point, which results in good interorbital nesting. We calculate the spin (charge) susceptibilities  $\hat{\chi}^{s(c)}(q)$  for  $q = (q, \omega_m = 2m\pi T)$  based on the random phase approximation (RPA). The spin Stoner factor  $\alpha_s$  is

defined as the maximum eigenvalue of  $\hat{\Gamma}^s \hat{\chi}^0(q, 0)$ , where  $\hat{\Gamma}^{s(c)}$  is the bare Coulomb interaction for the spin (charge) channel, and  $\hat{\chi}^0$  is the irreducible susceptibilities given by the Green's function without self-energy  $\hat{G}(k) = [(i\epsilon_n - \mu)\hat{1} - \hat{h}^0(k)]^{-1}$  for  $n = [k, \epsilon_n = (2n + 1)\pi T]$ . Since the relation  $\hat{\chi}^s(q) \propto \frac{1}{1 - \alpha_s}$  holds, spin fluctuations become large with increasing  $\alpha_s$  ( $\propto r$ ), and  $\alpha_s = 1$  corresponds to the spin-ordered state. Here,  $\hat{h}^0(k)$  is the matrix expression of  $H^0$  and  $\mu$  is the chemical potential. Details of  $\hat{\Gamma}^{s(c)}$ ,  $\hat{\chi}^{s(c)}(q)$ , and  $\hat{\chi}^0(q)$  are presented in SM A [45]. We fix the parameters  $r = 0.303$  in the BaFe<sub>2</sub>As<sub>2</sub> model unless otherwise noted. In this case,  $\alpha_s = 0.96$  at  $T = 30$  meV, and the averaged intraorbital Coulomb interaction is  $rU \sim 1.6$  eV. Figure 1(c) shows the obtained spin susceptibilities  $\chi^s_{4,4;4,4}(q, 0)$  and  $\chi^s_{3,4;3,4}(q, 0)$ , the peaks of which at  $q = (0, \pi)$  originate from the intraorbital (4-4) and the interorbital (3-4) nesting, respectively.  $\chi^s_{4,4;4,4}$  is larger than  $\chi^s_{3,3;3,3}$  because of the good intra- $d_{xy}$ -orbital nesting between e-FSS and h-FS3.

Hereafter, we study the symmetry breaking in the self-energy  $\hat{f}^q$  for wave vector  $q$  based on the density-wave (DW) equation introduced in Refs. [19, 32, 47]. We calculate both the momentum and orbital dependences of  $\hat{f}$  self-consistently to analyze both the orbital order and bond order on equal footing. To identify the realized DW with wave vector  $q$ , we solve the linearized DW equation,

$$\lambda_q f^q_{l,l'}(k) = \frac{T}{N} \sum_{k', m, m'} K^q_{l,l'; m, m'}(k, k') f^q_{m, m'}(k'), \quad (2)$$

where  $\lambda_q$  is the eigenvalue of the DW equation. The DW with wave vector  $q$  appears when  $\lambda_q = 1$ , and the eigenvector  $\hat{f}^q(k)$  gives the DW form factor. A larger value of  $\lambda_q$  corresponds to a more dominant DW state. Details of the kernel function  $\hat{K}^q(k, k')$  are given in SM A [45]. The Maki-Thompson (MT) terms and Aslamazov-Larkin (AL) terms shown in Fig. 1(d) are included in the kernel function. Near the magnetic criticality, the AL terms are strongly enhanced in proportion to  $\sum_p \chi^s(p) \chi^s(-p + q_c)$ , and they induce charge DW order through the three-boson coupling  $C_{Q_s, Q'_s}$  in Fig. 1(a).

Figure 2(a) shows the  $q$  dependences of  $\lambda_q$  for the total terms, the MT terms, and AL terms at  $T = 32.4$  meV.  $q = (0, \pi)$  AFB order appears at  $T^* = 32.4$  meV, while  $\lambda_0$  is slightly smaller than unity. Thus, the ferro-orbital transition temperature  $T_S$  is lower than  $T^*$ . The relation  $\lambda_{(0, \pi)} > \lambda_0$  is robust in the presence of moderate spin fluctuations  $\alpha_s \gtrsim 0.85$ . Both the AL and MT terms contribute to the AFB order cooperatively as shown in Fig. 2(a). Figure 2(b) shows the dominant component of the static form factor  $f^q_{3,4}(k)$  for  $q = (0, \pi)$ , which is derived from the analytic continuation of  $\hat{f}^q(k)$ . The other subdominant components are explained in SM B [45]. Focusing on the  $X$  and  $M$  points,  $f^q_{3,4}(k)$  is proportional to  $-\cos(k_y)$ , which corresponds to the interorbital AFB order shown in Fig. 2(c), where the  $y$ -direction hoppings between orbitals 3 and 4 are modulated by the correlation hopping  $\delta t_{3,4}(y; y \pm 1) = -\delta t_{4,3}(y; y \pm 1) = \delta t(-1)^y$ . Note that  $\delta t_{l,m}(y; y')$  is real and equal to  $\delta t_{m,l}(y'; y)$ .

The origin of the AFB order  $f^q_{3,4}(k)$  is the quantum interference between the antiferro-spin fluctuations  $\chi^s_{3,4;3,4}(Q)$  for  $Q \approx (0, \pi)$  and ferro-spin fluctuations  $\chi^s_{4,4;4,4}(0)$  shown in Fig. 1(a). The former is enhanced by the interorbital

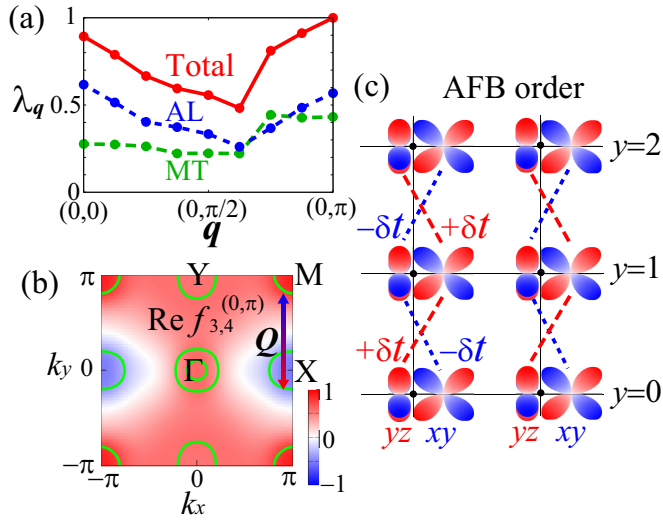


FIG. 2. (a) Obtained  $\mathbf{q}$  dependences of  $\lambda_{\mathbf{q}}$  at  $T = 32.4$  meV. The contributions from the AL and MT terms are also shown. (b) Dominant component of the form factor at  $\mathbf{q} = (0, \pi)$ ,  $f_{3,4}^{\mathbf{q}}(\mathbf{k})$ , which is given by the off-diagonal orbitals 3 and 4. The green lines indicate FSs. (c) Picture of the interorbital AFB order induced by  $f_{3,4}^{(0,\pi)}$ .

nesting shown in Fig. 1(b), while the latter  $\chi_{4,4;4,4}^s(\mathbf{0})$  is caused moderately by the forward intraorbital scattering of orbital 4 in h-FS3. The developments of  $\chi_{3,4;3,4}^s(\mathbf{Q})$  and  $\chi_{4,4;4,4}^s(\mathbf{0})$  are shown by the red dotted circle in Fig. 1(c). Moreover, the three-boson coupling  $C_{\mathbf{Q},\mathbf{Q}'}$  in Fig. 1(a) is strongly enlarged when  $\mathbf{q}_c = \mathbf{Q}_s + \mathbf{Q}'_s$  is a nesting vector [48], and this condition is satisfied when  $\mathbf{Q}_s = \mathbf{Q}$  and  $\mathbf{Q}'_s = \mathbf{0}$ . Thus,  $\lambda_{\mathbf{Q}}$  becomes large due to the AL terms. In addition to the AL terms, the MT terms strengthen the sign change of  $f_{3,4}^{(0,\pi)}(\mathbf{k})$  between the X and M points, as reported previously [19,32,49]. Thus, the AFB order originates from the cooperation between the AL and MT terms due to the interorbital nesting.

In contrast, the FO instability that corresponds to  $\lambda_{\mathbf{0}}$  originates mostly from the AL term owing to the combination of  $\chi_{3,3;3,3}^s(\mathbf{q})$  and  $\chi_{3,3;3,3}^s(-\mathbf{q})$  for  $\mathbf{q} \approx (\pi, 0)$ , as discussed in Refs. [17,18,20].

Here, we explain that a pseudogap originates from the band-folding driven band hybridization under the  $\mathbf{q} = (0, \pi)$  AFB order. Since the form factor grows in proportion to  $\text{Re}\sqrt{\lambda_{\mathbf{q}} - 1}$  in the Ginzburg-Landau theory, we introduce the mean-field-like  $T$ -dependent form factor  $\hat{f}^{\mathbf{q}}(T) = f^{\text{max}} \tanh(1.74\sqrt{T^*/T - 1})\hat{f}_{\text{DW}}^{\mathbf{q}}$ , where  $\hat{f}_{\text{DW}}^{\mathbf{q}}$  is the obtained form factor normalized as  $\max_{\mathbf{k}} |f_{\text{DW}}^{\mathbf{q}}(\mathbf{k})| = 1$ . We put  $f^{\text{max}} = 60$  meV. Details of the calculation method under the AFB order are explained in SM B [45]. Figure 3(a) shows the obtained DOS. For  $T < T^*$ , a pseudogap appears, which is consistent with the angle-resolved photoemission spectroscopy (ARPES) measurement [38]. Figures 3(b) and 3(c) show the FSs and spectral weight, respectively, under the  $\mathbf{q} = (0, \pi)$  AFB order at  $T = 28$  meV. Here, the folded band structure under the AFB order is unfolded to the original two-Fe Brillouin zone by following Ref. [50], which gives the spectrum corresponding to the ARPES measurements [38,39,51]. Owing to the band folding, several Dirac-type

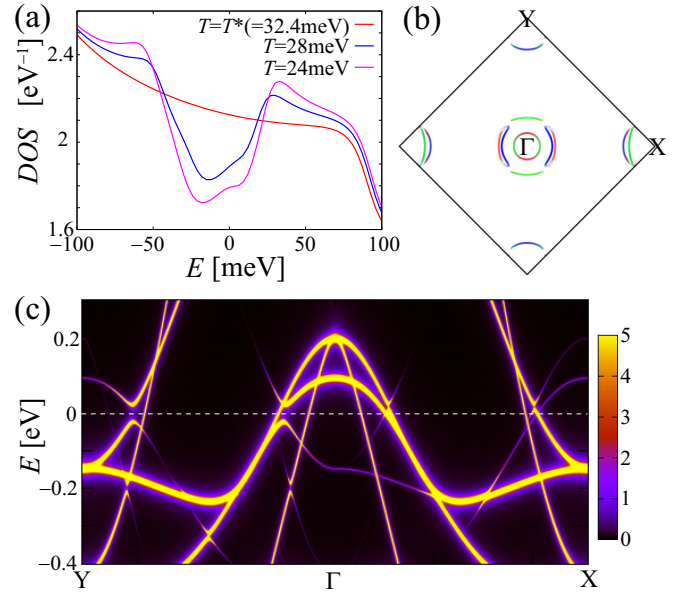


FIG. 3. (a) DOS at  $T = T^*(= 32.4$  meV), 28 meV, and 24 meV in the AFB state. Here, we introduced the quasiparticle damping  $\gamma = 10$  meV. (b) FSs and (c) spectral weight for  $\gamma = 1$  meV under  $\mathbf{q} = (0, \pi)$  AFB order at  $T = 28$  meV in the original two-Fe Brillouin zone.

band structures and shadow bands appear, as reported through an ARPES study [51].

In the following, we explain the “hidden nature” of the present AFB order, that is, the tiny anomalies in  $\chi^s(\mathbf{Q})$  and  $\chi_{\text{nem}}(\mathbf{0})$  at  $T^*$ . This is a long-standing mystery in Ba122. The  $T$  dependences of  $\alpha_s$  with and without  $\hat{f}^{(0,\pi)}(T)$  are shown in Fig. S2 in SM B [45]. The AFB order suppresses  $\alpha_s$  only slightly since the spin fluctuations are essentially intraorbital, while intraorbital components of  $\hat{f}^{(0,\pi)}(T)$  are subdominant. Next, we analyze the  $T$  dependencies of eigenvalue  $\lambda_{\mathbf{q}}$  for the FO order and AFB order by following SM B [45]. As shown in Fig. 4(a), the FO-order eigenvalue  $\lambda_{\mathbf{0}}$  is suppressed only slightly by the finite AFB order, owing to the slight decrease of  $\alpha_s$  and the “orbital selectivity” in nematicity: We stress that the dominant component of the form factor is different between the off-diagonal  $f_{3,4}^{(0,\pi)}$  in the AFB order and the diagonal  $f_{3,3(4,4)}^0$  ( $f_{3,4}^0 = 0$ ) in the FO order as shown in SM C [45]. Thus, neither  $\chi^s(\mathbf{Q}) \propto 1/(1 - \alpha_s)$  nor

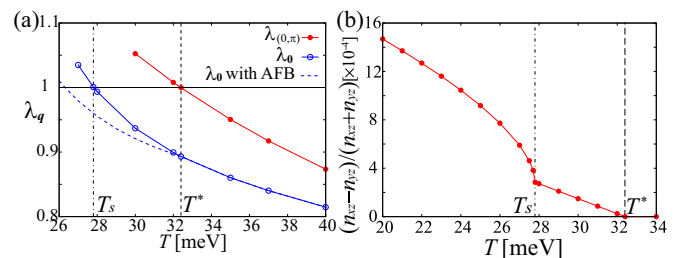


FIG. 4. (a)  $T$  dependencies of  $\lambda_{\mathbf{q}}$  for  $\mathbf{q} = (0, \pi)$  and  $\mathbf{q} = \mathbf{0}$ . The blue dotted line shows  $\lambda_{\mathbf{0}}$  with the AFB order for  $T < T^*$ . (b) The nematicity  $\psi = (n_2 - n_3)/(n_2 + n_3)$  including both AFB order for  $T < T^*$  and FO order for  $T < T_s$ .

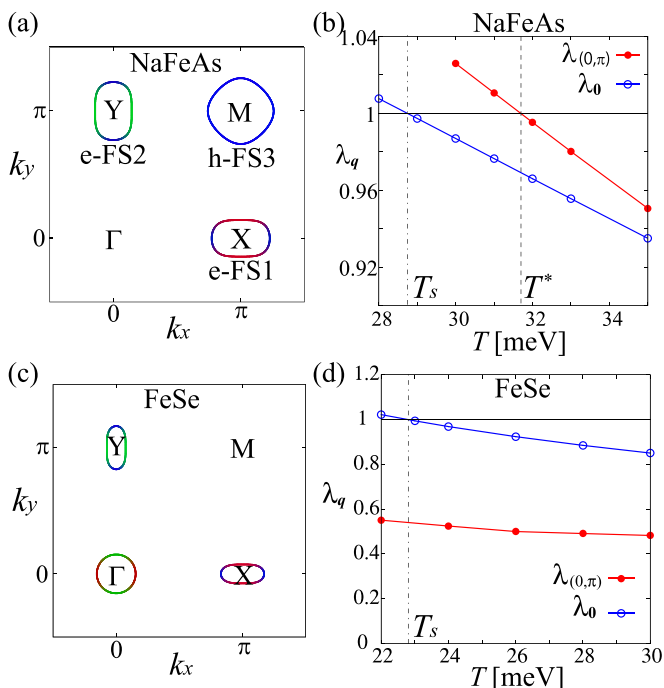


FIG. 5. (a) FSs of the NaFeAs model in the unfolded zone. (b)  $\lambda_q$  for  $\mathbf{q} = (0, \pi)$  and  $\mathbf{q} = \mathbf{0}$  in the NaFeAs model for  $r = 0.339$  ( $rU \sim 1.8$  eV). Then,  $\alpha_s = 0.92$  at  $T = 30$  meV. (c) FSs of the FeSe model. (d)  $\lambda_q$  in the FeSe model for  $r = 0.239$  ( $rU \sim 1.7$  eV). Then,  $\alpha_s = 0.85$  at  $T = 30$  meV.

$\chi_{\text{nem}}(\mathbf{0}) \propto 1/(1 - \lambda_0)$  would show a visible anomaly at  $T^*$ , which is consistent with experiments. (Here, the increment of  $T_S$  due to the electron-phonon interaction is not considered for simplicity.) In contrast, the FO order at  $T_S$  causes a sizable anomaly for  $\chi^s(\mathbf{Q})$  and  $\chi_{\text{nem}}(\mathbf{0})$ .

Another long-standing mystery is the  $T$ -linear behavior of nematicity  $\psi$  in Ba122 [34] and NaFeAs [40] below  $T^*$ . In order to solve this mystery, we calculate the  $T$  dependence of nematicity  $\psi = (n_2 - n_3)/(n_2 + n_3)$  in Fig. 4(b), where both  $\hat{f}^{(0,\pi)}(T)$  for  $T < T^*$  and the FO order  $\hat{f}^0(T)$  for  $T < T_S$  are introduced. For  $T < T_S$ , we assume  $\hat{f}^0(T) = f^{\text{max}} \tanh(1.74\sqrt{T_S/T - 1})\hat{f}_{\text{DW}}^0$ , where  $\hat{f}_{\text{DW}}^0$  is the obtained form factor normalized as  $\max_{\mathbf{k}} |\hat{f}_{\text{DW}}^0(\mathbf{k})| = 1$ . Details of  $\hat{f}_{\text{DW}}^0$  are presented in SM C [45]. We employ  $f^{\text{max}} = 60$  meV, which corresponds to the energy split  $\sim 60$  meV in the ARPES measurements [1]. Because the AFB order only slightly suppresses the FO-order transition as shown in Fig. 4(a), the obtained multistage nematic transitions are naturally expected in Ba122. The  $T$ -linear behavior  $\psi \propto (T^* - T)$  for  $T_S < T < T^*$  is a consequence of the relation  $\psi \propto [f^{(0,\pi)}(T)]^2$  because the  $f^{(0,\pi)}$  term cannot contribute to any  $\mathbf{q} = \mathbf{0}$  linear response. Note that the form factor  $\hat{f}^{(\pi,0)}$  for  $\mathbf{q} = (\pi, 0)$  gives  $\psi < 0$ . Thus, the  $T$ -linear behavior of  $\psi$  below  $T^*$  is also naturally explained by the AFB order. On the other hand,  $\psi \propto \sqrt{T_S - T}$  for  $T < T_S$  is induced by the FO order. To summarize, long-standing mysteries in the hidden nematic phase, such as tiny

anomalies in  $\chi^s(\mathbf{Q})$  and  $\chi_{\text{nem}}(\mathbf{0})$  at  $T^*$  and a  $T$ -linear  $\phi$  below  $T^*$ , are naturally explained in the present AFB-order scenario.

Finally, we discuss the universality of the hidden nematic order by focusing on NaFeAs and FeSe. According to the ARPES measurement in NaFeAs [52,53], only a single hole band mainly composed of a  $d_{xy}$  orbital crosses the Fermi level, resulting from the spin-orbit interaction (SOI)-induced band hybridization. To reproduce the single  $d_{xy}$ -orbital-like hole pocket in NaFeAs, we introduce the NaFeAs model without SOI by shifting downward the  $d_{xz}$  and  $d_{yz}$  hole bands immediately below the Fermi level in the BaFe<sub>2</sub>As<sub>2</sub> model. The FSs in the NaFeAs model are shown in Fig. 5(a). Details of the model are presented in SM A [45]. The obtained  $T$  dependences of  $\lambda_q$  in Fig. 5(b) are similar to those in the BaFe<sub>2</sub>As<sub>2</sub> model. The AFB order in NaFeAs is naturally understood as a consequence of the interorbital nesting between h-FS3 and e-FSs, as we discussed above. The FO order is driven by the spin fluctuations on the  $d_{xz}$  and  $d_{yz}$  orbitals. They are not weak because the top of the  $d_{xz}$  and  $d_{yz}$ -orbital hole band in NaFeAs is very close to the Fermi level according to the ARPES measurements [52,53]. The derived multistage nematic transition is consistent with the experiment on NaFeAs [40]. On the other hand, the  $d_{xy}$ -orbital hole pocket is missing in the FeSe model shown in Fig. 5(c). Because the interorbital nesting is missing,  $\lambda_{(0,\pi)}$  in the FeSe model is considerably smaller than unity as shown in Figs. 5(d) and S4(b) in SM D [45], which is consistent with the absence of the hidden nematic order in FeSe [43].

In this numerical study, we neglected the self-energy. However, the results are essentially unchanged if the self-energy is incorporated into the DW equation, as we verified in SM E [45]: We incorporate the self-energy into the DW equation in the framework of the conserving approximation, where the macroscopic conservation laws are satisfied rigorously and unphysical results are avoided.

In summary, we demonstrated that the origin of the hidden nematic state for  $T_S < T < T^*$  in BaFe<sub>2</sub>As<sub>2</sub> and NaFeAs, which is a long-standing unsolved problem, is naturally explained as the AFB ordered state. The tiny  $T$ -linear nematicity  $\psi = (n_{xz} - n_{yz})/(n_{xz} + n_{yz})$  as well as the emergence of the pseudogap and shadow band are naturally explained based on the present scenario. The phase diagrams of Ba122 and NaFeAs are understood by the present multistage nematic transition scenario. In contrast, the hidden nematic order is absent in FeSe because of the absence of the  $d_{xy}$ -orbital hole pocket.

Finally, we stress that the bond fluctuations significantly contribute to the pairing mechanism, as explained in SM F [45]. We will discuss this pairing mechanism in detail in future publications.

We are grateful to Y. Yamakawa for useful discussions. This work was supported by Grants-in-Aid for Scientific Research from MEXT, Japan (No. JP19H05825, No. JP18H01175, and No. JP17K05543)

[1] M. Yi, D. H. Lu, J.-H. Chu, J. G. Analytis, A. P. Sorini, A. F. Kemper, B. Moritz, S.-K. Mo, R. G. Moore, M. Hashimoto,

W.-S. Lee, Z. Hussain, T. P. Devereaux, I. R. Fisher, and Z.-X. Shen, *Proc. Natl. Acad. Sci. USA* **108**, 6878 (2011).



- [2] M. Yoshizawa, D. Kimura, T. Chiba, S. Simayi, Y. Nakanishi, K. Kihou, C.-H. Lee, A. Iyo, H. Eisaki, M. Nakajima, and S. Uchida, *J. Phys. Soc. Jpn.* **81**, 024604 (2012).
- [3] A. E. Böhmer, P. Burger, F. Hardy, T. Wolf, P. Schweiss, R. Fromknecht, M. Reinecker, W. Schranz, and C. Meingast, *Phys. Rev. Lett.* **112**, 047001 (2014).
- [4] Y. Gallais, R. M. Fernandes, I. Paul, L. Chauviere, Y.-X. Yang, M.-A. Measson, M. Cazayous, A. Sacuto, D. Colson, and A. Forget, *Phys. Rev. Lett.* **111**, 267001 (2013).
- [5] Y. Hu, X. Ren, R. Zhang, H. Luo, S. Kasahara, T. Watashige, T. Shibauchi, P. Dai, Y. Zhang, Y. Matsuda, and Y. Li, *Phys. Rev. B* **93**, 060504(R) (2016).
- [6] R. M. Fernandes, L. H. VanBebber, S. Bhattacharya, P. Chandra, V. Keppens, D. Mandrus, M. A. McGuire, B. C. Sales, A. S. Sefat, and J. Schmalian, *Phys. Rev. Lett.* **105**, 157003 (2010).
- [7] R. M. Fernandes, E. Abrahams, and J. Schmalian, *Phys. Rev. Lett.* **107**, 217002 (2011).
- [8] F. Wang, S. A. Kivelson, and D.-H. Lee, *Nat. Phys.* **11**, 959 (2015).
- [9] R. Yu and Q. Si, *Phys. Rev. Lett.* **115**, 116401 (2015).
- [10] J. K. Glasbrenner, I. I. Mazin, H. O. Jeschke, P. J. Hirschfeld, and R. Valenti, *Nat. Phys.* **11**, 953 (2015).
- [11] C. Fang, H. Yao, W.-F. Tsai, J. P. Hu, and S. A. Kivelson, *Phys. Rev. B* **77**, 224509 (2008).
- [12] R. M. Fernandes and A. V. Chubukov, *Rep. Prog. Phys.* **80**, 014503 (2017).
- [13] F. Krüger, S. Kumar, J. Zaanen, and J. van den Brink, *Phys. Rev. B* **79**, 054504 (2009).
- [14] W. Lv, J. Wu, and P. Phillips, *Phys. Rev. B* **80**, 224506 (2009).
- [15] C.-C. Lee, W.-G. Yin, and W. Ku, *Phys. Rev. Lett.* **103**, 267001 (2009).
- [16] H. Kontani, T. Saito, and S. Onari, *Phys. Rev. B* **84**, 024528 (2011).
- [17] S. Onari and H. Kontani, *Phys. Rev. Lett.* **109**, 137001 (2012).
- [18] S. Onari, Y. Yamakawa, and H. Kontani, *Phys. Rev. Lett.* **112**, 187001 (2014).
- [19] S. Onari, Y. Yamakawa, and H. Kontani, *Phys. Rev. Lett.* **116**, 227001 (2016).
- [20] Y. Yamakawa, S. Onari, and H. Kontani, *Phys. Rev. X* **6**, 021032 (2016).
- [21] S. Onari and H. Kontani, in *Iron-Based Superconductivity*, edited by P. D. Johnson, G. Xu, and W.-G. Yin (Springer, Berlin, 2015).
- [22] K. Jiang, J. Hu, H. Ding, and Z. Wang, *Phys. Rev. B* **93**, 115138 (2016).
- [23] L. Fanfarillo, G. Giovannetti, M. Capone, and E. Bascones, *Phys. Rev. B* **95**, 144511 (2017).
- [24] A. V. Chubukov, M. Khodas, and R. M. Fernandes, *Phys. Rev. X* **6**, 041045 (2016).
- [25] B. A. Frandsen, E. S. Bozin, H. Hu, Y. Zhu, Y. Nozaki, H. Kageyama, Y. J. Uemura, W.-G. Yin, and S. J. L. Billinge, *Nat. Commun.* **5**, 5761 (2014).
- [26] G. Zhang, J. K. Glasbrenner, R. Flint, I. I. Mazin, and R. M. Fernandes, *Phys. Rev. B* **95**, 174402 (2017).
- [27] H. Nakaoka, Y. Yamakawa, and H. Kontani, *Phys. Rev. B* **93**, 245122 (2016).
- [28] M. Tsuchiizu, K. Kawaguchi, Y. Yamakawa, and H. Kontani, *Phys. Rev. B* **97**, 165131 (2018).
- [29] J. Li, D. Zhao, Y. P. Wu, S. J. Li, D. W. Song, L. X. Zheng, N. Z. Wang, X. G. Luo, Z. Sun, T. Wu, and X. H. Chen, [arXiv:1611.04694](https://arxiv.org/abs/1611.04694).
- [30] X. Liu, R. Tao, M. Ren, W. Chen, Q. Yao, T. Wolf, Y. Yan, T. Zhang, and D. Feng, *Nat. Commun.* **10**, 1039 (2019).
- [31] K. Ishida, M. Tsujii, S. Hosoi, Y. Mizukami, S. Ishida, A. Iyo, H. Eisaki, T. Wolf, K. Grube, H. v. Löhneysen, R. M. Fernandes, and T. Shibauchi, *Proc. Natl. Acad. Sci. USA* **117**, 6424 (2020).
- [32] S. Onari and H. Kontani, *Phys. Rev. B* **100**, 020507(R) (2019).
- [33] V. Borisov, R. M. Fernandes, and R. Valenti, *Phys. Rev. Lett.* **123**, 146402 (2019).
- [34] S. Kasahara, H. J. Shi, K. Hashimoto, S. Tonegawa, Y. Mizukami, T. Shibauchi, K. Sugimoto, T. Fukuda, T. Terashima, A. H. Nevidomskyy, and Y. Matsuda, *Nature (London)* **486**, 382 (2012).
- [35] Y. K. Kim, W. S. Jung, G. R. Han, K.-Y. Choi, C.-C. Chen, T. P. Devereaux, A. Chainani, J. Miyawaki, Y. Takata, Y. Tanaka, M. Oura, S. Shin, A. P. Singh, H. G. Lee, J.-Y. Kim, and C. Kim, *Phys. Rev. Lett.* **111**, 217001 (2013).
- [36] E. Thewalt, I. M. Hayes, J. P. Hinton, A. Little, S. Patankar, L. Wu, T. Helm, C. V. Stan, N. Tamura, J. G. Analytis, and J. Orenstein, *Phys. Rev. Lett.* **121**, 027001 (2018).
- [37] T. Shimojima *et al.* (unpublished).
- [38] T. Shimojima, T. Sonobe, W. Malaeb, K. Shinada, A. Chainani, S. Shin, T. Yoshida, S. Ideta, A. Fujimori *et al.*, *Phys. Rev. B* **89**, 045101 (2014).
- [39] T. Shimojima, W. Malaeb, A. Nakamura, T. Kondo, K. Kihou, C.-H. Lee, A. Iyo, H. Eisaki, S. Ishida, M. Nakajima, S. Uchida, K. Ohgushi, K. Ishizaka, and S. Shin, *Sci. Adv.* **3**, e1700466 (2017).
- [40] R. Zhou, L. Y. Xing, X. C. Wang, C. Q. Jin, and G.-Q. Zheng, *Phys. Rev. B* **93**, 060502(R) (2016).
- [41] X. Ren, L. Duan, Y. Hu, J. Li, R. Zhang, H. Luo, P. Dai, and Y. Li, *Phys. Rev. Lett.* **115**, 197002 (2015).
- [42] H. Man, R. Zhang, J. T. Park, X. Lu, J. Kulda, A. Ivanov, and P. Dai, *Phys. Rev. B* **97**, 060507(R) (2018).
- [43] T. Shimojima, Y. Suzuki, T. Sonobe, A. Nakamura, M. Sakano, J. Omachi, K. Yoshioka, M. Kuwata-Gonokami, K. Ono, H. Kumigashira, A. E. Böhmer, F. Hardy, T. Wolf, C. Meingast, H. V. Löhneysen, H. Ikeda, and K. Ishizaka, *Phys. Rev. B* **90**, 121111(R) (2014).
- [44] H. Nakaoka, Y. Yamakawa, and H. Kontani, *Phys. Rev. B* **98**, 125107 (2018).
- [45] See Supplemental Material at <http://link.aps.org/supplemental/10.1103/PhysRevResearch.2.042005> for details of the models, formulation, tiny anomaly of  $\alpha_c$  at  $T^*$ , form factor of FO order, FO order without mass-enhancement factor in FeSe, conserving approximation, and pairing interaction by the AFB fluctuations.
- [46] T. Miyake, K. Nakamura, R. Arita, and M. Imada, *J. Phys. Soc. Jpn.* **79**, 044705 (2010).
- [47] K. Kawaguchi, M. Tsuchiizu, Y. Yamakawa, and H. Kontani, *J. Phys. Soc. Jpn.* **86**, 063707 (2017).
- [48] Y. Yamakawa and H. Kontani, *Phys. Rev. Lett.* **114**, 257001 (2015).
- [49] R. Q. Xing, L. Classen, and A. V. Chubukov, *Phys. Rev. B* **98**, 041108(R) (2018).
- [50] W. Ku, T. Berlijn, and C.-C. Lee, *Phys. Rev. Lett.* **104**, 216401 (2010).

- [51] A. Fujimori (private communication).
- [52] M. Yi, D. H. Lu, R. G. Moore, K. Kihou, C.-H. Lee, A. Iyo, H. Eisaki, T. Yoshida, A. Fujimori, and Z.-X. Shen, *New J. Phys.* **14**, 073019 (2012).
- [53] M. D. Watson, S. Aswartham, L. C. Rhodes, B. Parrett, H. Iwasawa, M. Hoesch, I. Morozov, B. Büchner, and T. K. Kim, *Phys. Rev. B* **97**, 035134 (2018).